ISSN 1674-1056
http://cpb.iphy.ac.cn
http://iopscience.iop.org/cpb
中国物理 B
Chinese Physics
中国物理 Chinese Physics B

Selective enhancement of green upconversion luminescence of Er-Yb: $NaYF_4$ by surface plasmon resonance of $W_{18}O_{49}$ nanoflowers and applications in temperature sensing

Ang Li(李昂), Jin-Lei Wu(吴金磊), Xue-Song Xu(许雪松), Yang Liu(刘洋), Ya-Nan Bao(包亚男), Bin Dong(董斌)

Citation: Chin. Phys. B . 2018, 27(9): 097301. **doi:** 10.1088/1674-1056/27/9/097301

Journal homepage: http://cpb.iphy.ac.cn; http://iopscience.iop.org/cpb

What follows is a list of articles you may be interested in

Optical interaction between one-dimensional fiber photonic crystal microcavity and gold nanorod

Yang Yu(于洋), Ting-Hui Xiao(肖廷辉), Zhi-Yuan Li(李志远)

Chin. Phys. B . 2018, 27(1): 017301. **doi:** 10.1088/1674-1056/27/1/017301

Tunable multiple plasmon resonances and local field enhancement of nanocrescent/nanoring structure

Wang Bin-Bing, Zhou Jun, Chen Dong, Fang Yun-Tuan, Chen Ming-Yang

Chin. Phys. B . 2015, 24(8): 087301. **doi:** 10.1088/1674-1056/24/8/087301

Deep-ultraviolet surface plasmon resonance of Al and Al_{core}/Al_2O_{3shell} nanosphere dimers for surface-enhanced spectroscopy

Ci Xue-Ting, Wu Bo-Tao, Song Min, Chen Geng-Xu, Liu Yan, Wu E, Zeng He-Ping

Chin. Phys. B . 2014, 23(9): 097303. **doi:** 10.1088/1674-1056/23/9/097303

Fano-like resonance characteristics of asymmetric Fe_2O_3@Au core/shell nanorice dimer

Wang Bin-Bing, Zhou Jun, Zhang Hao-Peng, Chen Jin-Ping

Chin. Phys. B . 2014, 23(8): 087303. **doi:** 10.1088/1674-1056/23/8/087303

High-order plasmon resonances in an Ag/Al_2O_3 core/shell nanorice

Chen Li, Wei Hong, Chen Ke-Qiu, Xu Hong-Xing

Chin. Phys. B . 2014, 23(2): 027303. **doi:** 10.1088/1674-1056/23/2/027303

SPECIAL TOPIC — Nanophotonics

Selective enhancement of green upconversion luminescence of Er–Yb: $NaYF_4$ by surface plasmon resonance of $W_{18}O_{49}$ nanoflowers and applications in temperature sensing*

Ang Li(李昂)[1,2,3], Jin-Lei Wu(吴金磊)[2,3], Xue-Song Xu(许雪松)[1,2,†], Yang Liu(刘洋)[3], Ya-Nan Bao(包亚男)[2,3], and Bin Dong(董斌)[3,‡]

[1] School of Chemistry and Chemical Engineering, Liaoning Normal University, Dalian 116029, China
[2] Department of Physics, Dalian Maritime University, Dalian 116026, China
[3] Key Laboratory of Photosensitive Materials and Device of Liaoning Province, Key Laboratory of New Energy and Rare Earth Resource Utilization of State Ethnic Affairs Commission, School of Physics and Materials Engineering, Dalian Minzu University, Dalian 116600, China

(Received 11 May 2018; revised manuscript received 5 July 2018; published online 28 August 2018)

The $W_{18}O_{49}$ nanoflowers with a diameter of 500 nm are prepared by a facile hydrothermal method. The Er–Yb: $NaYF_4$ nanoparticles are adsorbed on the petals (the position of the strongest local electric field on $W_{18}O_{49}$ nanoflowers). With a 976 nm laser diode (LD) as an excitation source, the selectively green upconversion luminescence (UCL) is observed to be enhanced by two orders of magnitude in Er–Yb: $NaYF_4/W_{18}O_{49}$ nanoflowers heterostructures. It suggests that the near infrared (NIR)-excited localized surface plasmon resonance (LSPR) of $W_{18}O_{49}$ is primarily responsible for the enhanced UCL, which could be partly reabsorbed by the $W_{18}O_{49}$, thus leading to the selective enhancement of green UCL for the Er–Yb: $NaYF_4$. The fluorescence intensity ratio is investigated as a function of temperature based on the intense green UCL, which indicates that Er–Yb: $NaYF_4/W_{18}O_{49}$ nanoflower heterostructures have good potential for developing into temperature sensors.

Keywords: upconversion, localized surface plasmon resonance, Er–Yb: $NaYF_4/W_{18}O_{49}$, temperature sensing

PACS: 73.20.Mf, 78.68.+m, 65.80.–g, 68.55.–a **DOI:** 10.1088/1674-1056/27/9/097301

1. Introduction

In the past few decades, a great deal effort has been devoted to the upconversion (UC) luminescence of rare-earth ions doped materials because of their wide applications.[1–7] The $NaYF_4$ has been regarded as the most efficient UC matrix due to its low phonon energy and crystalline surrounding.[8–10] Although recent advances in synthesis have led to the accurate control of morphology, crystal phase, and emission colors, it is still difficult to obtain highly efficient upconversion nanoparticles. Research has been performed to improve the luminescent efficient of UC materials, such as adding different sensitizers,[11,12] changing the environment of the luminous center,[13,14] enhancing the local optical field by surface plasmon of noble metal-nanostructures,[15,16] etc. Plasmonic modulation of noble metal nanoparticles is a promising method of improving UC luminescence of nanophosphors.[2,15,16] Plasmonic nanostructures can concentrate the incoming light into a strong localized electric field distributed within a subwavelength region close to the surface of the nanostructures.[17–19] However, the widespread application has been seriously limited due to the high-cost noble metal. Recently, some heavily doped semiconductors, such as Sn-doped In_2O_3, WO_{3-x}, $Cu_{2-x}S$, and MoO_{3-x}, have been demonstrated to show the localized surface plasmon resonance (LSPR) phenomena.[20–24] Among them, the blue WO_{3-x}, a kind of nonstoichiometric tungsten oxide, exhibits an intense LSPR absorption in both the visible region and the near infrared (NIR) region.[21,25]

In this paper, we report a flower-like $W_{18}O_{49}$ prepared by the hydrothermal method. The Er–Yb: $NaYF_4$ nanoparticles are adsorbed at the tips of petals, which are the position of the strongest local electric field. More than one order of magnitude UC enhancement is achieved through this structure. In addition, its temperature sensing property is also studied.

2. Experimental details

2.1. Materials

All chemicals were obtained from commercial suppliers and used without further purification. All reagents were of analytical grade. Rare earth chloride $ReCl_3 \cdot 6H_2O$ (*Re* is Y, Yb, Er, 99.9%, respectively) were purchased from Aladdin Chem-

*Project supported by the National Natural Science Foundation of China (Grant Nos. 11474046 and 61775024), the Program for Liaoning Innovation Team in University, China (Grant No. LT2016011), the Science and Technique Foundation of Dalian, China (Grant Nos. 2017RD12 and 2015J12JH201), and the Fundamental Research Funds for the Central Universities, China (Grant No. DC201502080203).

†Corresponding author. E-mail: xuxuesong@dlmu.edu.cn
‡Corresponding author. E-mail: dong@dlnu.edu.cn

© 2018 Chinese Physical Society and IOP Publishing Ltd

istry Co. Ltd in Shanghai, China. Oleic acid (OA, $C_{18}H_{34}O_2$, 90%) and octadecene (ODE, $C_{18}H_{36}$, 90%) were purchased from Alfa Aesar. Hexacarbonyl tungsten ($W(CO)_6$) was purchased from Sigma–Aldrich. Sodium hydroxide (NaOH, $\geq$ 98%) and ammonium fluoride (NH_4F, A.R.) were purchased from Sinopharm Chemical Reagent Co. Ltd in Shanghai, China.

2.2. Sample preparation

2.2.1. Synthesis of $W_{18}O_{49}$ nanoflowers

In a typical process, 30 mg of $W(CO)_6$ was dissolved into 20 mL of absolute ethanol with constant stirring to form a yellow transparent solution. Then, the solution was transferred to a 50 mL teflon-lined stainless steel autoclave, and heated up to 200 °C and kept for 10 h. The produced samples were separated from the solution by centrifugation, washed with ethanol three times, and dried in a vacuum oven.

2.2.2. Synthesis of Er–Yb: $NaYF_4$ nanoparticles

In a typical synthesis of 20 nm nanoparticles, 1 mmol of rare earth chlorate (Y/Yb/Er = 78:20:2) with 6 mL of oleic acid and 15 mL of 1-octadecene was added into a 100 mL flask to form a mixed solution with vigorous stirring under the vacuum condition. The solution was heated to 100 °C and kept for 30 min and then cooled down to 50 °C to dissolve the rare earth. Then a methanol solution (10 mL) containing NH_4F (4 mmol) and NaOH (2.5 mmol) was added dropwise, and the resulting solution was kept at 100 °C for 30 min. After methanol was evaporated, the solution was heated to 305 °C under an argon atmosphere and kept for 90 min and then cooled down to room temperature. The nanoparticles were precipitated by the addition of ethanol and isolated via centrifugation. The resulting product was washed three times with cyclohexane and ethanol (1:3) and finally dispersed into cyclohexane at a concentration of about 0.1 M.

2.2.3. Synthesis of Er–Yb: $NaYF_4/W_{18}O_{49}$ nanoflowers heterostructures

The 3 mg of $W_{18}O_{49}$ nanoflowers and 0.1 mL of Er–Yb: $NaYF_4$ suspended cyclohexane solution (0.1 M) were dropped into 20 mL of cyclohexane solution under ultrasonic treatment for 3 h. After that the resulting sample was separated from the solution by centrifugation, and then dried in a vacuum oven.

2.2.4. Synthesis of Er–Yb: $NaYF_4/WO_3$ nanoflowers up-conversion luminescence particles

The dried $W_{18}O_{49}$ nanoflower samples were placed in a muffle furnace, ashing at 500 °C for 2 h to obtain WO_3. The resulting sample was washed three times with ethanol and dried in a vacuum oven. The Er–Yb: $NaYF_4/WO_3$ nanoflowers were synthesized by using the same procedure mentioned above.

2.3. Characterization

The phase structures of the Er–Yb: $NaYF_4$ and Er–Yb: $NaYF_4/W_{18}O_{49}$ nanoflowers heterostructures were analyzed by a SHIMADZU XRD-6000 x-ray diffractometer (XRD) with Cu $K\alpha$ radiation, by using the scanning mode in 2θ ranging from 10° to 80° in steps of 0.02° and at a rate of 4.0 °/min. The surface morphology of the phosphors was observed using a Hitachi S-4800 scanning electron microscope (SEM) at an acceleration voltage of 5 kV. The UV/visible/NIR absorption spectra of the samples were measured by a Lambda 750 (Perkin Elmer) combined with an integrating sphere. The UC emission properties of the products were measured by a microscope (Olympus IX71) combined with a spectrometer (PI Instrument). The excitation with a 976-nm laser passing through a laser clean-up was reflected into the objective (50× Olympus) by a dichroic short pass filter. The UC emission was collected by the same objective and led into the spectrometer. The laser clean-up and dichroic filter were used to purify the excitation light and eliminate the laser line before the emission was detected. The optical images were achieved under 976-nm irradiation by an Olympus microscope (Scheme 1). The UC emissions from the samples at different temperatures were focused onto a Jobin Yvon iHr550 monochromator and detected with a CR131 photomultiplier tube under a 976 nm LD excitation. A home-made temperature controlling system was used to adjust the temperature of the samples from room temperature to 650 K, in which the measuring and controlling accuracy of temperature was about ±0.5 K.

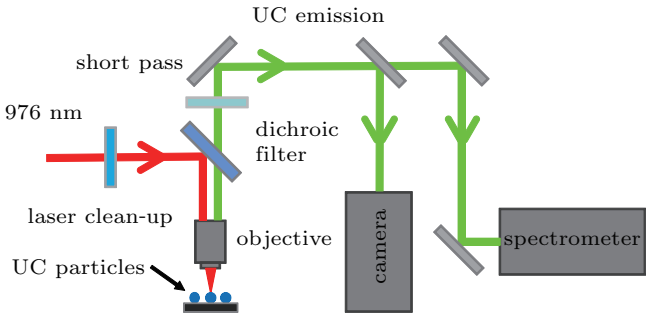


Fig. 1. (color online) Schematic illustration of the set-up used to measure UC emissions of as-fabricated products.

3. Results and discussion

The surface morphologies of $W_{18}O_{49}$, Er–Yb: $NaYF_4$, and Er–Yb: $NaYF_4/W_{18}O_{49}$ nanoflowers heterostructures are shown in Figs. 2(a)–2(d). The $W_{18}O_{49}$ nanoflowers are well-distributed and show uniform size with the average particle diameter about 500 nm (Fig. 2(a)). There are about 40 petals distributed evenly in all directions in one $W_{18}O_{49}$ nanoflower. The tip of the petal is about 120 nm long. Figure 2(b) shows that the Er–Yb: $NaYF_4$ nanoparticles are monodispersed, and the average diameter of the nanoparticles is around 20 nm. The petals of $W_{18}O_{49}$ nanoflowers are filled with Er–Yb: $NaYF_4$

nanoparticles. The Er–Yb: $NaYF_4$ nanoparticles are adsorbed at the tips of petals (Figs. 2(c) and 2(d)).

Figure 2(e) shows the XRD patterns of the Er–Yb: $NaYF_4/W_{18}O_{49}$ nanoflowers heterostructures. The XRD pattern of the Er–Yb: $NaYF_4/W_{18}O_{49}$ nanoflower heterostructure is well indexed, corresponding well to the standard pattern of the hexagonal phase of $NaYF_4$ (JCPDS No. 16-334) and $W_{18}O_{49}$ (JCPDS No. 71-2450). There are no other diffraction peaks, indicating that $NaYF_4$ and $W_{18}O_{49}$ nanoflowers coexist in the Er–Yb: $NaYF_4/W_{18}O_{49}$ nanoflower heterostructure and do not change their phase. In Fig. 2(f), the $W_{18}O_{49}$ nanoflower shows an intrinsic absorption edge around 410 nm. Besides, a very broad absorption band ranging from 450 nm to the near-infrared spectrum region is detected on the $W_{18}O_{49}$ nanoflower, which can be assigned to the metal-like LSPR induced by the collective oscillations of excess charges (electrons) on the surface of tungsten oxide due to the abundant oxygen vacancies. The broad absorption band of the $W_{18}O_{49}$ nanoflower can improve the absorption and emission process. So it is obvious that the combination of plasmonic $W_{18}O_{49}$ nanoflowers and Er–Yb: $NaYF_4$ nanoparticles can result in a UC luminescence enhancement within the noble metal-free structure.

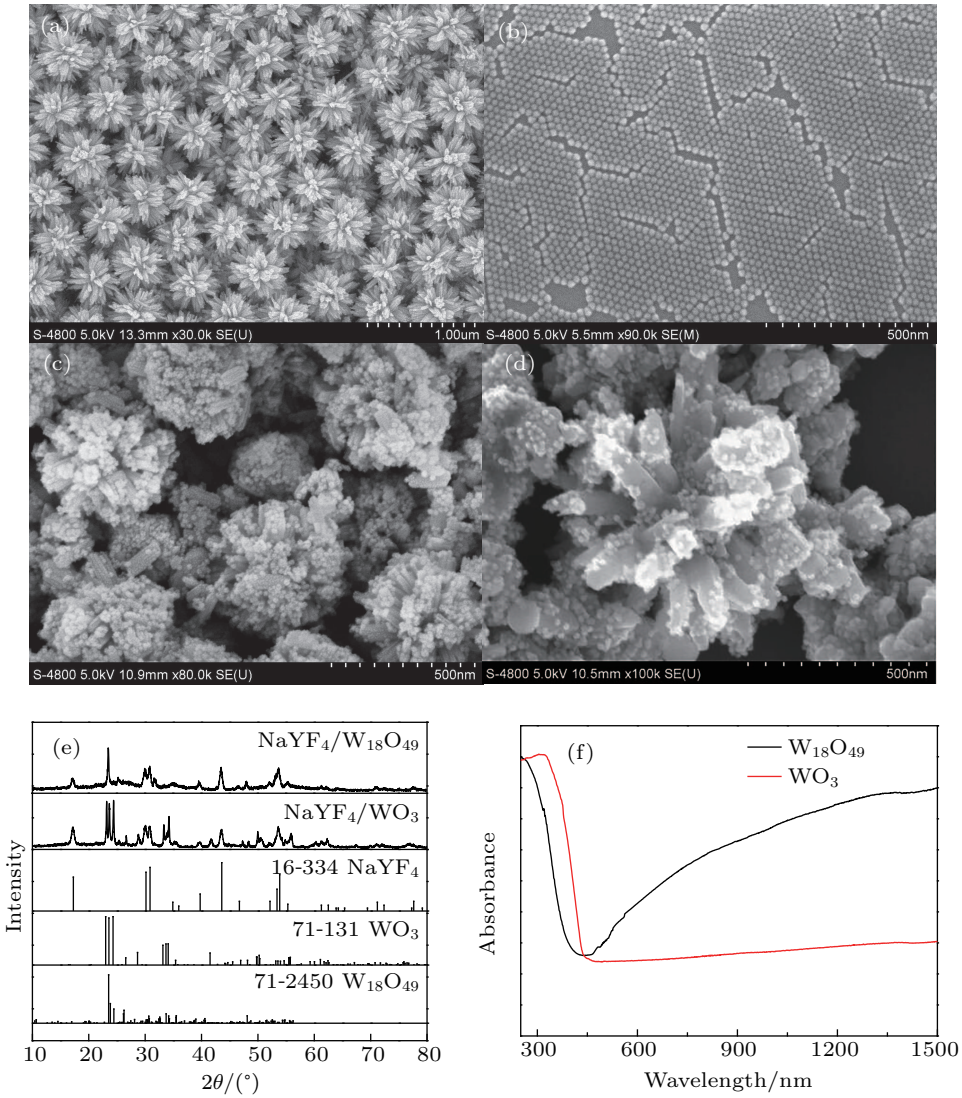


Fig. 2. (color online) SEM images of (a) $W_{18}O_{49}$ nanoflowers, (b) Er–Yb: $NaYF_4$ particles, (c) Er–Yb: $NaYF_4/W_{18}O_{49}$ nanoflowers particles, and (d) Er–Yb: $NaYF_4/W_{18}O_{49}$ nanoflowers particles; (e) XRD patterns of Er–Yb: $NaYF_4/W_{18}O_{49}$ and Er–Yb: $NaYF_4/WO_3$ nanoflowers particles; and (f) absorption spectra of $W_{18}O_{49}$ and WO_3 nanoflowers.

Figure 3(a) shows the UC emission spectra of Er–Yb: $NaYF_4/W_{18}O_{49}$ nanoflower heterostructures and Er–Yb: $NaYF_4$ nanoparticles under 976 nm LD excitation. The green and red UC emissions originating from the transitions of $^2H_{11/2}/^4S_{3/2} \rightarrow {}^4I_{15/2}$ and $^4F_{9/2} \rightarrow {}^4I_{15/2}$ are observed between 500 nm and 580 nm and between 620 nm and 700 nm, respectively. Neither the band position of green emission nor the band position of red emission shows any change after combination of plasmonic $W_{18}O_{49}$ nanoflowers and Er–Yb: $NaYF_4$ nanoparticles. The intensity of green emission is enhanced by

about 13 fold. However, the red emission is reduced by about 5 fold. The selective enhancement of green upconversion luminescence may be due to the interaction between $W_{18}O_{49}$ nanoflowers and Er–Yb: $NaYF_4$ nanoparticles. Figure 3(b) shows the dependence of the green UC emission intensity on the excitation power of Er–Yb: $NaYF_4/W_{18}O_{49}$ nanoflower heterostructures. It is known that for an unsaturated UC process, the number of photons which are required to populate the upper emitting state can be obtained by $I_{up} \propto I_{pump}^{n}$, where I_{up} is the UC emission intensity, I_{pump} is the pump laser power, and n is the number of laser photons required.[26] The value of n in the transition of green emission is 2.03, which indicates that the two-photon process is mainly responsible for the green UC emission of Er–Yb: $NaYF_4/W_{18}O_{49}$ nanoflower heterostructures.

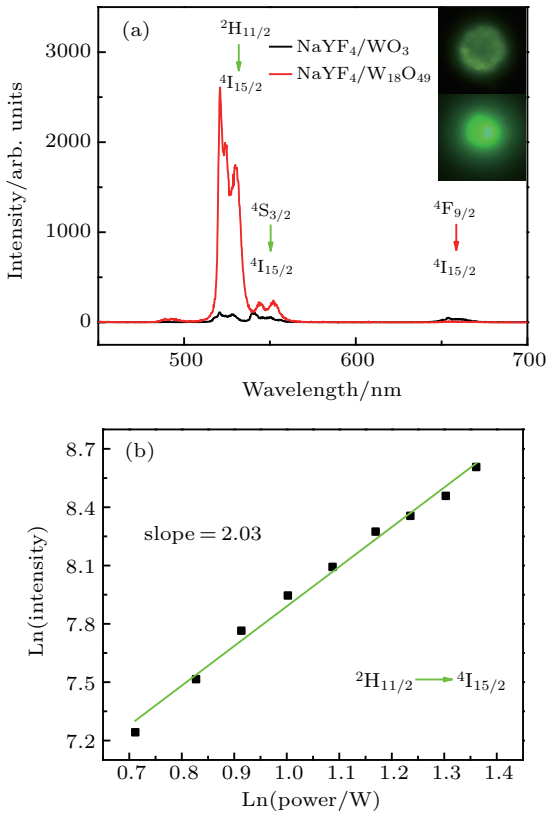


Fig. 3. (color online) (a) The UC emission spectra of Er–Yb: $NaYF_4/W_{18}O_{49}$ nanoflowers particles and Er–Yb: $NaYF_4$ nanoparticles under 976 nm LD excitation. (b) Plot of logarithmic green UC emission intensity versus logarithmic excitation power of pump laser for Er–Yb: $NaYF_4/W_{18}O_{49}$ nanoflowers particles.

Figure 4 shows the schematic energy levels diagram of Er–Yb: $NaYF_4/W_{18}O_{49}$ nanoflower heterostructure under 976 nm LD excitation. The Yb^{3+} is excited to the $^2F_{5/2}$ level by ground state absorption. The two emitting levels of $^2H_{11/2}$ and $^4S_{3/2}$ that produce green UC emissions by transition of $^2H_{11/2}/^4S_{3/2} \rightarrow {}^4I_{15/2}$ are mainly populated by the sequential energy transfers and the nonradiative relaxations from $^4F_{7/2}$ to $^2H_{11/2}$ and $^4S_{3/2}$ levels. The population of $^4F_{9/2}$ that emits red emission by the transition of $^4F_{9/2} \rightarrow {}^4I_{15/2}$ is mainly ascribed to the cross relaxation and subsequent energy transfer process. The 976 nm laser can excite both Er–Yb: $NaYF_4$ nanoparticles and the LSPR of $W_{18}O_{49}$ nanoflowers, leading the UC luminescence to increase by 13 fold. The $W_{18}O_{49}$ nanoflowers can concentrate the near-infrared light on the surface and transmit the energy to Er–Yb: $NaYF_4$ nanoparticles by resonance energy transfer. So the Er–Yb: $NaYF_4$ nanoparticles at the interface of Er–Yb: $NaYF_4/W_{18}O_{49}$ nanoflower heterostructure will have an intensive interaction with $W_{18}O_{49}$ nanoflowers.

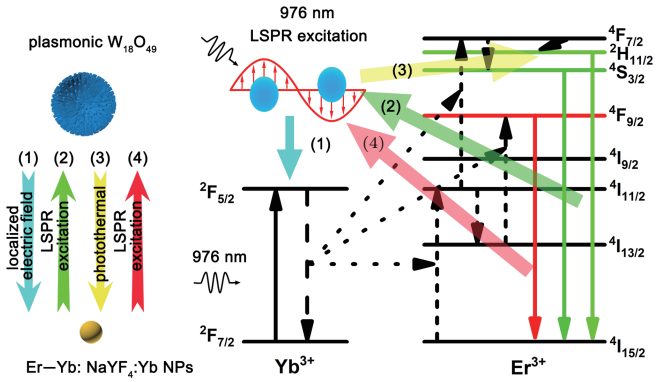


Fig. 4. (color online) Schematic energy level diagram of Er–Yb: $NaYF_4/W_{18}O_{49}$ up-conversion luminescence nanoflowers particles under 976 nm LD excitation.

The temperature-dependent UC luminescence property is important for understanding the luminescent physical mechanism and the practical application of UC materials. Figure 5(a) shows the green UC luminescence spectra for Er–Yb: $NaYF_4/W_{18}O_{49}$ nanoflowers heterostructures at the temperatures of 350 K, 550 K, and 625 K, respectively. With the increase of temperature, none of the band positions of green emissions change, however, the fluorescence intensity ratios between the two emissions vary. With the thermalization of populations at the coupled energy levels of $^2H_{11/2}$ and $^4S_{3/2}$, the populations of the two pairs of energy levels follow Boltzmann's distribution and the fluorescence intensity ratio (FIR) between the two green UC emissions of the $^2H_{11/2} \rightarrow {}^4I_{15/2}$ and $^4S_{3/2} \rightarrow {}^4I_{15/2}$ transitions can be expressed as

$$\mathrm{FIR} = R = \frac{I_H}{I_S} = \frac{N(^2H_{11/2})}{N(^4S_{3/2})} = C\exp\left(\frac{-\Delta E}{kT}\right), \qquad (1)$$

where I_H and I_S are the integrated intensities of the transitions $^2H_{11/2} \rightarrow {}^4I_{15/2}$ and $^4S_{3/2} \rightarrow {}^4I_{15/2}$, respectively, and ΔE is the energy gap between the coupled energy levels of $^2H_{11/2}$ and $^4S_{3/2}$. Pre-exponential factor C is a constant relating to the states degeneracy, emission cross-section, and angular frequency of the corresponding transitions. Figure 5(b) shows a plot of the logarithmic FIR of green UC emissions at 522 nm and 546 nm versus inverse absolute temperature in a range of 325–625 K. The experimental data are fitted to a straight line with a slope of about 609.3. The FIR between green upconversion emissions at 522 nm and 546 nm relative to the temperature range of 325–625 K is shown in Fig. 5(c). The coefficient C in Eq. (1) is 6.28 according to the fitting curve of the experimental data.

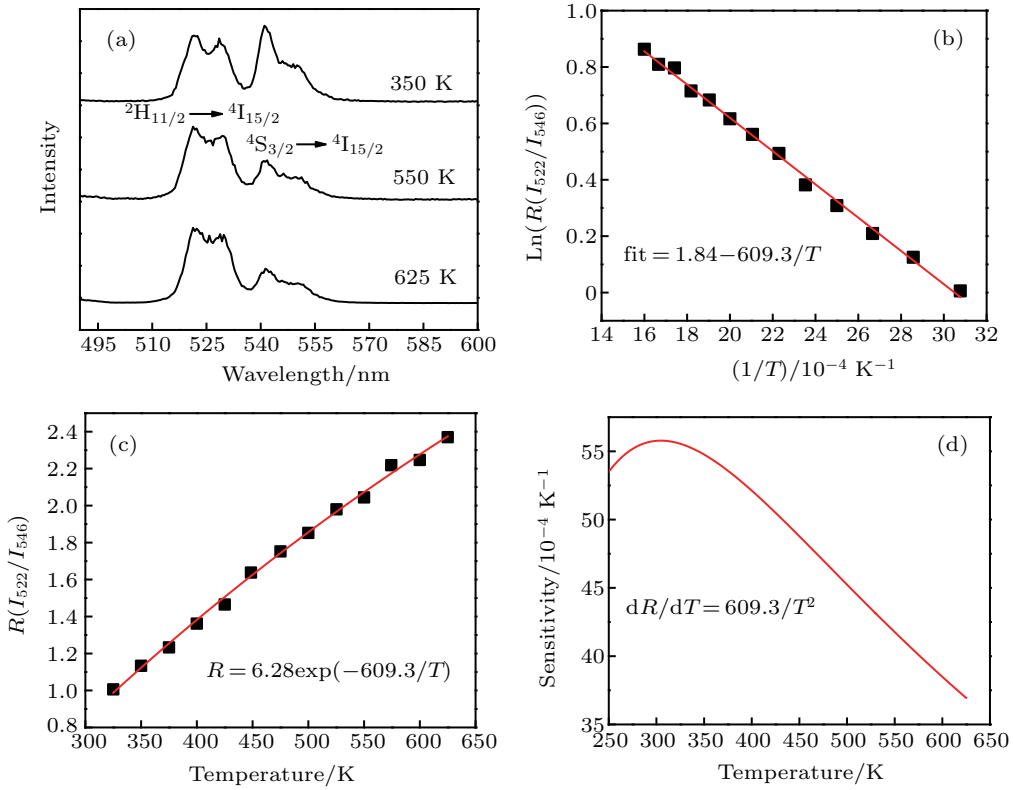


Fig. 5. (color online) (a) Green UC emission spectra of Er–Yb: $NaYF_4/W_{18}O_{49}$ up-conversion luminescence nanoflower particles at 350 K, 550 K, and 625 K. (b) Plot of logarithmic FIR versus inverse absolute temperature. (c) FIR of the $^2H_{11/2}/^4S_{3/2} \rightarrow {}^4I_{15/2}$ transitions as a function of temperature. (d) Sensor sensitivity as a function of temperature in a range of 250–625 K.

With regard to optical temperature-sensing applications, it is extremely important to know that the sensitivity varies with temperature. The sensor sensitivity can be defined as[23]

$$S = \frac{\mathrm{d}R}{\mathrm{d}T} = R\frac{\Delta E}{kT^2}. \tag{2}$$

At a temperature of 305.17 K, the sensitivity of the Er–Yb: $NaYF_4/W_{18}O_{49}$ nanoflowers heterostructure attains its maximum value of approximately 0.0056 K^{-1} as shown in Fig. 5(d). The results prove that the Er–Yb: $NaYF_4/W_{18}O_{49}$ nanoflower heterostructures have potential for developing into temperature sensors.

4. Conclusion

In this research, $W_{18}O_{49}$ nanoflowers have been successfully synthesized by using a facile hydrothermal method. The nanoflowers show uniform size with the average particle diameter about 500 nm. About 40 petals are distributed evenly in all directions in one $W_{18}O_{49}$ nanoflower and the tip of the petal is about 120 nm long. The UC luminescence property of Er–Yb: $NaYF_4/W_{18}O_{49}$ nanoflower heterostructure is studied under 976 nm excitation. The UC luminescence is increased by 13 fold. It suggests that the NIR-excited LSPR of $W_{18}O_{49}$ is primarily responsible for the enhanced UC luminescence, which can be partly absorbed by the $W_{18}O_{49}$, thus leading to the selective enhancement of green UC luminescence for the Er–Yb: $NaYF_4$. The FIR of green UC is investigated as a function of temperature, demonstrating that the Er–Yb: $NaYF_4/W_{18}O_{49}$ nanoflower heterostructures have potential for being developed into temperature sensors.

References

[1] Liu Q, Li F, Shen Z, Yang T, Yang Y, Yao P and Yin B 2013 *J. Am. Chem. Soc.* **135** 5029
[2] Yin Z, Li H, Xu W, Cui S, Zhou D, Chen X, Zhu Y, Qin G and Song H 2016 *Adv. Mater.* **28** 2518
[3] Dong B, Cao B, He Y, Liu Z, Li Z and Feng Z 2012 *Adv. Mater.* **24** 1987
[4] Wei T, Dong Z, Zhao C Z, Ma Y J, Zhang T B, Xie Y F, Zhou Q J and Li Z P 2016 *Ceram. Int.* **42** 5537
[5] He E J, Liu N, Zhang M L, Qin Y F, Guan B G, Li Y and Guo M L 2012 *Chin. Phys. B* **21** 073201
[6] Gao W and Dong J 2017 *Acta Phys. Sin.* **66** 204206 (in Chinese)
[7] Yang Y X, Xu Z, Zhao S L, Liang Z Q, Zhu W and Zhang J J 2017 *Chin. Phys. B* **26** 087801
[8] Generalova A N, Rocheva V V, Nechaev A V, Khochenkov D A, Sholina N V, Semchishen V A, Zubov V P, Koroleva A V, Chichkov B N and Khaydukov E V 2016 *Rsc. Adv.* **6** 30089
[9] Li Z H, Park W, Zorzetto G, Lemaire J S and Summers C J 2014 *Chem. Mater.* **26** 1770
[10] Wang J, Song H, Xu W, Dong B, Xu S, Chen B, Yu W and Zhang S 2013 *Nanoscale* **5** 3412
[11] Cao B S, Wu J L, Feng Z Q and Dong B 2013 *Mater. Chem. Phys.* **142** 333
[12] Marciniak L, Bednarkiewicz A, Stefanski M, Tomala R, Hreniak D and Strek W 2016 *J. Mater. Chem. C* **4** 2513
[13] Wang F, Han Y, Lim C S, Lu Y, Wang J, Xu J, Chen H, Zhang C, Hong M and Liu X 2010 *Nature* **463** 1061
[14] Cao B S, Wu J L, Wang X H, Feng Z Q and Dong B 2016 *J. Nanosci. Nanotechnol.* **16** 3690

[15] Greybush N J, Saboktakin M, Ye X, Della G C, Oh S J, Berry N E, Engheta N, Murray C B and Kagan C R 2014 *ACS Nano* **8** 9482

[16] Yin Z, Zhou D, Xu W, Cui S, Chen X, Wang H, Xu S and Song H 2016 *ACS. Appl. Mater. Inter.* **8** 11667

[17] Hartl G V 2011 *Chem. Rev.* **111** 3858

[18] Olson J, Dominguezmedina S, Hoggard A, Wang L Y, Chang W S and Link S 2015 *Chem. Soc. Rev.* **44** 40

[19] Schuller J A, Barnard E S, Cai W, Jun Y C, White J S and Brongersma M L 2010 *Nat. Mater.* **9** 193

[20] Kanehara M, Koike H, Yoshinaga T and Teranishi T 2009 *J. Am. Chem. Soc.* **131** 17736

[21] Zhang Z Y, Jiang X Y, Liu B K, Guo L J, Lu N, Wang L, Huang J D, Liu K C and Dong B 2018 *Adv. Mater.* **30** 1705221

[22] Mocatta D, Cohen G, Schattner J, Millo O, Rabani E and Banin U 2011 *Science* **332** 77

[23] Cheng H, Kamegawa T, Mori K and Yamashita H 2014 *Angew. Chem. Int. Edit.* **53** 2910

[24] Chen Y, Liu X C, Chen W D, Xie Z W, Huang Y R and Li L 2017 *Chin. Phys. B* **26** 017807

[25] Zhang Z Y, Huang J D, Fang Y R, Zhang M Y, Liu K C and Dong B 2017 *Adv. Mater.* **29** 1606688

[26] Pollnau M, Gamelin D R, Uuml S R, Uuml T U and Hehlen M P 2000 *Phys. Rev. B* **61** 3337